Phytoplankton competition, cell-to-cell spacing, and biodiversity

8 November 2024

Classification: Biological Sciences

Key Words: Phytoplankton, Biodiversity, Competition

Abstract

Competition for resources is viewed as foundational to species exclusion and community structuring. The decades-old 'R* rule' emerging from phytoplankton competition experiments states that the species able to maintain steady-state biomass at the lowest resource level (R*) will outcompete all other species. However, the notion of resource-based competitive exclusion is clearly violated within natural phytoplankton assemblages that consistently exhibit coexisting species with vastly different resource acquisition potentials. Here, we explain (1) the critical difference between laboratory competition experiments and natural plankton systems, (2) how predator-prey relationships prevent superior resource competitors from excluding inferior competitors, (3) why the 'R* rule' is not valid for these systems, (4) the relevance of cell-to-cell spacing to competition, (5) how resource inventories structure plankton communities, and (6) why diversity within ecological niches created by predator-prey pairs is theoretically unconstrained. Our findings likely apply to other ecological communities with strong predator-prey coupling.

Significance Statement

Traditional laboratory phytoplankton competition experiments show that the species able to maintain steady-state biomass at the lowest resource level will outcompete all other species limited by that resource (referred to as the 'R* rule') and that the number of stably coexisting species is equal to the number of different limiting resources. These conclusions are inconsistent with natural phytoplankton assemblages with diverse, coexisting species having vastly different resource acquisition potentials. Here we explain how "ecological niches" created by predator-prey relationships, spatial distancing between cells, and rapid resource recycling allow for the stable coexistence of rich phytoplankton biodiversity. Our findings offer an ecosystem-based framework to improve understanding of natural plankton communities and their representation in ecological models.

Introduction

For over a century, the Darwinian view of resourced-based competition between individuals leading to exclusion of species [1,2] has guided our interpretation of the natural world. With respect to phytoplankton, Evelyn Hutchinson [3] famously stated, "*The problem that is presented…is essentially how it is possible for a number of species to coexist in a…unstructured environment all competing for the same sorts of materials. … According to the principle of competitive exclusion, we should expect that one species alone would outcompete all the others…*" Beginning in the 1970's, laboratory phytoplankton competition experiments provided strong support for this notion [4-10] by demonstrating that the outcome of a competition could be predicted based on *a priori* knowledge of relationships between nutrient concentration and uptake for two competing species. From this emerged the 'R* rule' stating that, for a common limiting resource, the species that can achieve a steady-state population at the lowest resource level (denoted R*) will outcompete all other species [5,11]. The long-standing focus on resource competition in phytoplankton ecology is woven into how we construct and interpret ecosystem models and in our predictions of change under a warming climate. It is also at odds with field observations. Spanning from the most nutrient-depleted 'oligotrophic' waters to nutrient-rich 'eutrophic' waters, measurements consistently demonstrate diverse populations of coexisting phytoplankton species with dramatically different resource acquisition potentials [12-14] (Fig. 1a). A provocative proposal to explain this inconsistency is that phytoplankton in nature are too distantly spaced to allow the type of resourced-based competitive exclusion exhibited in laboratory experiments [15-18]. Here, we describe the role of intercellular spacing in phytoplankton community structuring, explain why the 'R* rule' does not hold, provide a conceptual framework with elements of strong competition that enables stable coexistence of diverse phytoplankton species, and propose that this conception may be applicable to other ecological systems.

RESULTS

From oligotrophic to eutrophic waters, neighboring phytoplankton cells in the open ocean are separated on average by ~100 to 400 body lengths [19]. Nutrient uptake by these cells results in a depletion zone referred to as the 'diffusive boundary layer' that extends to approximately nine

times a cell's diameter [20], beyond which nutrient concentrations are essentially equivalent to that of the bulk media (S_∞) (Fig. 2b). For natural communities of nutrient-limited phytoplankton, the vast intercellular spacing implies that boundary layers rarely overlap between cells, but these boundary layers are still interlinked through nutrient diffusion. An intuitive analogy of this link between distantly spaced phytoplankton is provide by water level regulation in Lake Berryessa, California [21]. In this analogy, the 'Glory Hole' spillway represents a phytoplankton cell and the depression of water around this spillway is the boundary layer (Fig. 2a). Despite its meager cross-sectional area, the 'Glory Hole' can maintain a constant water level across the entire 80 km^2 lake surface (Fig. 2b) because a strong force (i.e., gravity) rapidly eliminates gradients in water elevation. Indeed, if the lake's surface is two meters above the spillway when it is opened, the time required for the 'Glory Hole' (maximum flow rate ~1400 m^3 s^{-1}) to drop the lake level to 1 m above the spillway ($t_{1/2}$) is a mere 16 h [21]. For phytoplankton, the 'strong force' tending to homogenize resource concentrations between cells is obviously not gravity, but rather diffusion.

In the oligotrophic central ocean gyres, nitrogen is often the limiting resource for phytoplankton growth [22,23], with total concentrations of biologically available forms (e.g., NO_3, NO_2, NH_4) typically ranging from S_∞ = 3 to 17 nM [19]. Phytoplankton communities in these waters exhibit steep size distributions with slopes of −4 to -4.5 between the logarithm of cell number concentration per unit length and the logarithm of cell diameter (d) [12-14,24] (e.g., Fig. 1a). The most abundant taxon in ocean gyres is *Prochlorococcus* (d = 0.6 μm) and, at cell concentrations ranging from 2×10^4 to 2×10^5 cell ml^{-1} [19,25], these populations can potentially decrease the forestated S_∞ values by 50% in $t_{1/2}$ = 4.5 to 5.8 h (Supporting Information Fig. 1, Supporting Discussion). Values of $t_{1/2}$ for the second most abundant taxon, *Synechococcus* (d = 1.5 μm), and larger cells range from ~1 day to many months, respectively (Supporting Information Fig. 1). These time scales illustrate the strongly size-dependent potential for diffusion-based uptake to deplete resources far beyond the boundary layers of cells. Importantly, they are also comparable to (or much longer than) nutrient recycling times in quasi-steady-state plankton systems. Since mechanisms of recycling are often spatially discrete (e.g., zooplankton excretion), they further suggest a potential for resource patchiness on very short time scales.

Figure 2c expands upon the Lake Berryessa analogy by considering a hypothetical lake with multiple spillways (A_1, B_1, B_2) representing 3 phytoplankton cells of two species (A, B), where the height of each spillway is inversely proportional to water drainage capacity (i.e., representing nutrient affinity differences between species) (Fig. 2c). With a high initial lake level (dashed surface in Fig. 2c), all three spillways contribute to lake drainage but, in time, spillway A_1 (e.g., *Prochlorococcus*) 'competitively excludes' both B spillways (e.g., larger diatoms) because the former spillway can drain the lake below the intake levels of the latter (Fig. 2c). This is the essence of the 'R* rule' and it is independent of the spacing between spillways (i.e., cells).

What happens to the above lake analogies of resource-based competitive exclusion if it is raining? Rainfall to the Lake Berryessa drainage basin causes $t_{1/2}$ to increase and, if this water inflow is ~1400 $m^3\ s^{-1}$, then $t_{1/2} \rightarrow \infty$ and the 'Glory Hole' can no longer control the level of the lake. This scenario is depicted in figure 1d where all the water passing through the spillways is redeposited on the lake's surface. Consequently, the lake level is not determined by the drawdown potential of the spillways, but rather by the total amount of water in the system. This condition is analogous to nutrient-limited quasi-steady-state phytoplankton communities. Spillway A_1 can still cause spillway B_1 to go 'extinct' because their boundary layers overlap, but spatial separation of A_1 and B_2 causes flow through these spillways to be independent and determined by their respective 'concentration gradients' (i.e., distance from the spillway lip to lake elevation) (Fig. 2d). Despite the simplicity of these analogies, the key take-home message here is that the concentration of limiting nutrient in the far-field between cells (S_∞) is not determined by the species that can maintain steady-state biomass at the lowest resource level but, rather, by the total amount of limiting resource in the system (which is dependent on the balance between external sources and losses). This is why natural phytoplankton populations do not obey the R* rule.

To better understand this vital conclusion, it is instructive to consider differences between laboratory competition experiments and natural plankton communities. In classic competition experiments [e.g., 4-6], culture media is inoculated with two phytoplankton species at concentrations below steady-state carrying capacity and then changes in each species' biomass (P) are monitored over time. As the experiment progresses, a fraction of the culture is removed

and replaced by fresh media at a predefined cadence (l; per unit time). The significance of this practice is that the removal of culture simulates perfectly neutral (i.e., species-independent) and linear (i.e., lP) predation. The winner of the competition is the species that can achieve a division rate (μ) equal to the predation rate at the highest steady-state biomass, which is equivalent to saying the species that can achieve $\mu = l$ at the lowest S_∞. As the superior competitor decreases S_∞, predation on the inferior competitor exceeds its division rate and it is washed out of the culture at the specific rate, $e^{-(l-\mu)t}$, where t = time [26]. This outcome is the same whether steady-state biomass is so high that diffusive boundary layers continuously overlap between cells (i.e., concentration of limiting resource in fresh media is very high) or so low that they rarely overlap (i.e., concentration of limiting resource in fresh media is very low) because diffusion rates are fast and simple linear predation on the superior competitor allows this species to reach a final steady state where μP (in units of limiting resource per time) equals the limiting resource resupply rate.

In nature, predation on phytoplankton is neither neutral nor linear. Rather, most zooplankton predators are size-specific in their prey selection [27-32] and their grazing rate is dependent on both phytoplankton concentration and their own abundance, which generally increases in parallel with prey abundance [33-35]. At quasi-steady state (e.g., ocean gyres), the balance between division and loss is such that no single predator-prey size class can reach a μP equal to the total limiting resource resupply rate. Instead, this resource is distributed across all predator-prey size classes in a manner proportional to the μ of each class, as dictated in part by boundary layer diffusion. Thus, the total supply rate of limiting resource is equal to the sum of μP for all size classes (as in the water recycling loop of Fig. 2d). This is the fundamental difference between laboratory competition experiments and natural plankton populations, and it implies that no phytoplankton size class can exclude another size class based on resource competition (contrary to the R* rule). It also implies that the smallest cells will dominate the phytoplankton community when the total inventory of limiting resource is particularly low (due to their faster diffusion-limited division rates) and that larger cells will increase in prominence as the resource inventory increases (due to their often-higher maximum division rate potentials paralleled by resource saturation of division in the smallest cells) [19]. Thus, phytoplankton size distributions become less steep as the total amount of limiting resource in the system increases.

The above conclusions can be explored using a simple ecosystem model for nitrogen-limited growth with 25 size classes of both phytoplankton (d = 0.6 to 134 µm) and zooplankton [19,36]:

$$\frac{dP_i^N}{dt} = \mu_i P_i^N - g_1 f_i Z_i^N P_i^N \quad (1a)$$

and

$$\frac{dZ_i^N}{dt} = g_1 g_2 f_i Z_i^N P_i^N - g_3 Z_i^N - g_4 f_i (Z_i^N)^2 \quad (1b)$$

where P_i^N is the nitrogen content (µmol L^{-1}) of the i^{th} phytoplankton size class, Z_i^N is the nitrogen content of zooplankton (µmol L^{-1}) grazing upon the i^{th} phytoplankton size class, μ_i is the diffusion-supported division rate (d^{-1}), f_i defines predation size ranges, and g_1 through g_4 are zooplankton grazing rate, ingestion efficiency, linear mortality rate, and density-dependent mortality rate, respectively (Methods). The nutrient resupply rate is equal to the sum of zooplankton egestion/sloppy feeding and mortality [i.e., $g_1(1-g_2) f_i Z_i^N P_i^N + g_3 Z_i^N + g_4 f_i (Z_i^N)^2$] (Fig. 3a, right axis). For nitrogen inventories (ΣN) ranging from 4 to 20 µM, this minimal equation set consistently predicts the stable coexistence of all 25 phytoplankton size classes (Fig. 3b, right axis) and it yields steady-state phytoplankton communities with size distribution slopes that steepen with decreasing ΣN (consistent with field observations) [12-14] (Fig. 3b, left axis). The model also predicts ocean gyre-type S_∞ values (3-17 nM) for ΣN of ~5 to 8 µM (Fig. 3a, left axis) and that, for all ΣN < 10 µM, more than 97% of the total nitrogen inventory is sequestered in biomass (~60% in phytoplankton, ~40% in zooplankton) (Fig. 3c). Thus, size-dependent predator-prey relationships permit coexistence of phytoplankton with vastly different resource acquisition potentials and determine the partitioning of limiting resource that ultimately defines S_∞.

DISCUSSION

Our findings have profound implications on understanding phytoplankton community structuring and biodiversity. A fundamental prediction of the R* rule is that the number of stably coexisting

species is equal to the number of different limiting resources [37-39], and diverse explanations have been proffered to accommodate greater diversity while maintaining the tenant of resource-based competitive exclusion [40-43]. Concepts presented herein instead portray plankton communities as being structured by predator-prey relationships. We achieve stable coexistence of all modelled phytoplankton size classes because each class is associated with its own set of predators, with each predator-prey set defining a unique 'ecological niche' [18,44]. Within these ecological niches, competition is severe and even minor differences in fitness will, over time, result in exclusion. In this system, however, 'fitness' is not determined solely by a species' ability to acquire a limiting resource but rather by the combination of adaptations defining its division-loss balance relative to that of other species within its ecological niche (Fig. 4) [45]. This distinction eliminates the R* restriction on the potential abundance of coexisting species and theoretically permits unconstrained stable diversity.

Competition within an ecological niche is an issue of investment strategy, where resources dedicated to one advantage are not available to invest in others. An incomplete list of investment options includes reduction in cell quotas for limiting resources (e.g., metabolic networking [46,47]), development of symbiotic relationships (e.g., nitrogen fixing bacteria) [48], opportunistic adaptions to exploit resource patchiness (e.g., chemotaxis [49], retention of excess photosynthetic capacity [50,51], luxury uptake [52-54], elevated maximum division rate [55]), enhanced resource affinity [4,5], allelopathy [56], mixotrophy [57], production of chemical grazing deterrents, armored cell walls (e.g., coccoliths, thecal plates, frustules), and grazer avoidance (swimming) [58], and adaptations reducing losses to pathogens (e.g., low maximum division rate potential preventing explosive increases in abundance [55]). In temporally varying environments, physiological adaptations enabling seasonal blooming [55] or resting spore formation [59,60] can also contribute to a species' retention in the community. The requirement for stable coexistence within an ecological niche is that each phytoplankton species has identical fitness when averaged over the timescale of exclusion [61], which can span years to decades for closely matched species [17,18]. The multi-dimensional landscape of investment options illustrated in figure 4 implies that diverse (infinite?) options may exist for achieving this fitness equality within an ecological niche.

Adherence to principles of resource-based competitive exclusion, particularly following publications on laboratory competition experiments, has nurtured an overwhelmingly 'bottom-up' (meaning a focus on factors regulating division rates) view in phytoplankton ecology. The vast spatial distancing between individual phytoplankton (in terms of body lengths) in natural populations has been recognized as relevant to competition potential [15-18], but this intercellular spacing is not what hinders competitive exclusion *per se* because diffusion rates are sufficiently fast that gradients in nutrient concentrations can potentially be abolished on relatively short time scales (Supporting Information Fig. 1). What makes resource-based competitive exclusion unlikely in natural communities is the tight coupling between phytoplankton division and loss rates and subsequent recycling of resources, as high predation rates prevent populations with superior resource affinities from consuming the entire pool of recycled limiting resource. The reason cell-to-cell spacing is relevant is that it ensures the division rate of most cells is controlled by the far-field nutrient concentration (S_∞) and not the depleted nutrient concentrations of boundary layers around neighboring cells.

In the depiction of phytoplankton community structuring promoted here, competitive exclusion is decided by all factors influencing the relative division-loss balance of species within an ecological niche (Fig. 4) [17,18,62-64], while differences in resource acquisition potentials are expressed through the relative distribution of resources between size-structured ecological niches (Fig. 3b, left axis). We expect the same mechanisms to structure quasi-steady-state light-limited phytoplankton communities (e.g., populations living at the bottom of the sunlit layer of ocean gyres), albeit with a size dependency governed by light-absorption capacities (a function of cellular cross-sectional area) rather than diffusion potential (a function of cellular volume). The requirement for time-averaged equal fitness in ecological niches implies elevated potentiality for stable biodiversity in variable environments (e.g., high latitudes), as temporal changes in growth conditions will continually shift the relative fitness of different species [3,24,55,65,66]. We propose that fitness equivalence in ecological niches is also a foundation in phytoplankton biogeography [67,68], where unique adaptions to a specific environment (e.g., physiological temperature optima, photosynthetic light harvesting structures optimized for perpetually low-light growth) drive competitive exclusion of less fit species. This mechanism for exclusion, however, still does not inherently constrain the potential stable biodiversity of an ecological

246 niche due to the plethora of factors defining division-loss balances of species (Fig. 4). Thus, it
247 seems the bigger mystery regarding ecological niches is why, after billions of years of evolution,
248 observed phytoplankton diversity is not greater? [35]. While a few contributing factors have
249 been proposed [e.g., 17,18], a complete answer to this question remains elusive.
250
251 The ability of predator-prey relationships to override the inevitable resource-based outcome of a
252 two species competition experiment has been demonstrated in phytoplankton cultures [69-73].
253 Here we explain why growth, loss, and recycling processes in nature prevent species exclusions
254 based on resource acquisition alone. Similar rules of community structuring will equally apply
255 to other aquatic and terrestrial ecosystems where unchecked proliferation of superior resource
256 competitors is prevented by tightly coupled predation [74-76]. For all such systems, abandoning
257 a bottom-up view in favor of an ecosystem-based view will nurture a more thorough
258 understanding of natural communities and how we represent them in ecological models [76].

METHODS

Ecosystem Modeling

Results presented in figure 3 are based on a one-dimensional "*idealized food-chain model*" originally developed by Ward et al. [36] and modified by Behrenfeld et al. [19]. The model includes 25 phytoplankton size-classes with diameters ranging from 0.6 µm to 135 µm, where cells in a given size class are 1.25 times larger than those in the class one size smaller. Each size class is initiated with a representative diatom and non-diatom, which are distinguished by the former being non-motile and vacuolated and the latter being motile and non-vacuolated (these properties impact diffusion as vacuolation increases the cell surface area per unit cytoplasmic volume while motility distorts the diffusive boundary layer around a cell; see Behrenfeld et al. [19] for full details). The model also includes 25 zooplankton size classes. Predators of phytoplankton and predators of zooplankton are assumed to consume prey over a feeding size range that is proportional to (f_i in Eq. 1a,b) their mean prey size. This proportionality factor is defined in our model as $f_i = 0.5$, meaning that a predator with a mean prey size of 80 µm will have a feeding range of 40 – 120 µm, while a predator with a mean prey size of 2 µm will have a feeding range of 1 – 3 µm [19,36,77]. The model is intended to characterize phytoplankton community composition under steady-state nitrogen-limited growth conditions and, thus, temporal environmental variability is not included. Division rate for each phytoplankton size class and phytoplankton type (μ_i in Eq. 1a) follows a size-dependent saturating function defined by diffusion rate and maximum potential division rate, as described in detail in Behrenfeld et al. [19]. Predation is dependent on prey abundance and described by a zooplankton grazing rate (g_1) of 3.24 m^3 $mmol^{-1}$ d^{-1}, an ingestion efficiency (g_2) of 0.5 (unitless), a non-grazing mortality rate (g_3) of 0.06 d^{-1}, and a density-dependent mortality rate (g_4) of 1.6 m^3 $mmol^{-1}$ d^{-1} [78,79]. Model runs correspond to steady-state nitrogen inventories (ΣN) of 4 to 20 µM and S_∞ values of 1 nM to 10 µM, with increments in S_∞ of 1 nM from 1 to 21 nM, ~ 8 nM from 21 to 500 nM, and ~ 1 µM from 1 to 10 µM. For all model runs, light levels are assumed constant and saturating for growth. Each model run is initiated with P_i^N = 0.18 mmol N m^{-3} for both the diatom and non-diatom phytoplankton and Z_i^N = 0.04 mmol N m^{-3} for all size classes and then executed until steady state is reached [19]. Size diversity for the steady-state populations was assessed as the number of size-classes remaining that contributed at least 0.0001% to total phytoplankton biomass [19].

References

1. Gause, G. Experimental analysis of Vito Volterra's mathematical theory of the struggle for existence. *Science* 79, 16–17 (1934).

2. Hardin, G. The competitive exclusion principle. *Science* 131, 1292–1297 (1960).

3. Hutchinson G. E. The paradox of the plankton. *Amer. Nat*. 95, 137-145 (1961).

4. Tilman, D. Resource competition between plankton algae: an experimental and theoretical approach. *Ecology* 58, 338-348 (1977).

5. Tilman, D. Tests of resource competition theory using four species of Lake Michigan algae. *Ecology* 62, 802-815 (1981).

6. Tilman, D. & Sterner, R. W. Invasions of equilibria: tests of resource competition using two species of algae. *Oecologia* 61,197-200 (1984).

7. Hu, S. & Zhang, D. Y. The effects of initial population density on the competition for limiting nutrients in two freshwater algae. *Oecologia* 96, 569-574 (1993).

8. Spijkerman, E. & Coesel, P. F. Competition for phosphorous among planktonic desmid species in continuous-flow culture. *J. Phycol.* 32, 939-948 (1996).

9. Grover, J. P. *Resource competition* (Vol. 19). Springer Science & Business Media (1997).

10. Wilson, J. B., Spijkerman, E. & Huisman, J. Is there really insufficient support for Tilman's R* concept? A comment on Miller et al. *Amer. Nat*. 169, 700-706 (2007).

11. Armstrong, R. A. & McGehee, R. Competitive exclusion. *Amer. Nat.* 115, 151-170 (1980).

12. Sheldon, R. W., Prakash, A. & Sutcliffe Jr, W. The size distribution of particles in the Ocean. *Limnol. Oceanogr.* 17, 327-340 (1972).

13. Huete-Ortega, M., Cermeno, P., Calvo-Díaz, A. & Maranon, E. Isometric size-scaling of metabolic rate and the size abundance distribution of phytoplankton. *Proc. Royal Soc. B* 279, 1815-1823 (2012).

14. Marañón, E. Cell size as a key determinant of phytoplankton metabolism and community structure. *Annu. Rev. Mar. Sci.* 7, 241–64 (2015).

15. Hulburt E. M. Competition for nutrients by marine phytoplankton in oceanic, coastal, and estuarine regions. *Ecology* 51, 475-484 (1970).

16. Siegel D. A. Resource competition in a discrete environment: Why are plankton distributions paradoxical? *Limnol. Oceanogr.* 43, 1133-1146 (1998).

17. Behrenfeld M. J., O'Malley, R., Boss, E., Karp-Boss, L. & Mundt, C. Phytoplankton biodiversity and the inverted paradox. *ISME Comm*. 1, 1-9 (2021).

18. Behrenfeld, M. J. & Bisson, K. M. Neutral theory and plankton biodiversity. *Ann. Rev. Mar. Sci*. 16, 283-305 (2024).

19. Behrenfeld M. J., Bisson, K. M., Boss, E., Gaube, P. & Karp-Boss, L. Phytoplankton community structuring in the absence of resource-based competitive exclusion. *Plos one* 17, e0274183 (2022).

20. Karp-Boss, L., Boss, E. & Jumars, P. A. Nutrient fluxes to planktonic osmotrophs in the presence of fluid motion. *Oceanogr. Mar. Biol.* 34, 71-108 (1996).

21. Ward, B. A. How phytoplankton compete for nutrients despite vast intercellular separation. *ISME Comm.* 4, p.ycae003 (2024).

22. Dugdale, R. C. & Goering, J. J. Uptake of new and regenerated forms of nitrogen in primary productivity. *Limnol. Oceanogr.* 12, 196-206 (1967).

23. Moore, C. M., Mills, M. M., Arrigo, K. R., Berman-Frank, I., Bopp, L., Boyd, P. W., Galbraith, E. D., Geider, R. J., Guieu, C., Jaccard, S. L. & Jickells, T. D. Processes and patterns of oceanic nutrient limitation. *Nature Geosci*. 6, 701-710 (2013).

24. Behrenfeld M. J., Boss E. S. & Halsey K. H. Phytoplankton community structuring and succession in a competition-neutral resource landscape. *ISME Comm*. 1, 1-8 (2021).

25. Partensky, F., Hess W. R. & Vaulot, D. Prochlorococcus, a marine photosynthetic prokaryote of global significance. *Microbiol. Mol. Biol. Rev.* 63, 106-127 (1999).

26. Smith, R.E. & Kalff, J. Competition for phosphorus among co-occurring freshwater phytoplankton. *Limnol. Oceanogr*. 28, 448-464 (1983).

27. Wirtz, K. W. Who is eating whom? Morphology and feeding type determine the size relation between planktonic predators and their ideal prey. *Mar. Ecol. Progr. Ser*. 445, 1-12 (2012).

28. Kiørboe, T. How zooplankton feed: Mechanisms, traits and trade-offs. *Biol. Rev.* 86, 311–339 (2011).

29. Hansen, B., Bjornsen P. K. & Hansen P. J. The size ratio between planktonic predators and their prey. *Limnol. Oceanogr.* 39, 395–403 (1994).

30. Sommer, U. & Sommer, F. Cladocerans versus copepods: The cause of contrasting top–down controls on freshwater and marine phytoplankton. *Oecologia* 147, 183–194 (2006).

31. Hébert, M-P., Beisner B. E. & Maranger, R. Linking zooplankton communities to ecosystem functioning: Toward an effect-trait framework. *J. Plankton Res.* 39, 3–12 (2017).

32. Fuchs H. L. & Franks P.J. Plankton community properties determined by nutrients and size-selective feeding. *Mar. Ecol. Prog. Ser.* 413, 1-15 (2010).

33. Harvey, H. W. The supply of iron to diatoms. *J. Mar. Biol. Assoc. United Kingdom*, 22, 205–219 (1937).

34. Nielsen, E.S., 1958. The balance between phytoplankton and zooplankton in the sea. *ICES J. Mar. Res.* 23, 178-188 (1958).

35. Sommer, U., Worm, B. & Sommer, U. *Competition and coexistence in plankton communities*. Springer Berlin Heidelberg, pp. 79-108, (2002).

36. Ward BA, Dutkiewicz S, Follows MJ. Modelling spatial and temporal patterns in size-structured marine plankton communities: top–down and bottom–up controls. J. Plankt. Res. 2014; 36: 1: 31-47.

37. Taylor, P. A. & Williams, P. L. Theoretical studies on the coexistence of competing species under continuous-flow conditions. *Can. J. Microbiol*. 21, 90-98 (1975).

38. Sommer, U. Comparison between steady state and nonsteady state competition: experiments with natural phytoplankton. *Limnol. Oceanogr.* 30, 335–346 (1985).

39. Rothhaupt, K. O. Mechanistic resource competition theory applied to laboratory experiments with zooplankton. *Nature* 333, 660–662 (1988).

40. Huisman, J. & Weissing, F. J. Biodiversity of plankton by species oscillations and chaos. *Nature* 402, 407-410 (1999).

41. Huisman, J. & Weissing, F. J. reply: Coexistence and resource competition. *Nature* 407, 694 (2000).

42. Scheffer, M., Rinaldi, S., Huisman, J. & Weissing, F. J. Why plankton communities have no equilibrium: solutions to the paradox. *Hydrobiologia* 491, 9-18 (2003).

43. Cropp, R. & Norbury, J. Comment on "The paradox of the 'paradox of the plankton'" by Record et al. *ICES J. Mar. Sci.* 71, 293-295 (2014).

44. Chesson, P. & Kuang, J. J. The interaction between predation and competition. *Nature* 456, 235-238 (2008).

45. Holm, N. P. & Armstrong, D. E. Role of nutrient limitation and competition in controlling the populations of *Asterionella formosa* and *Microcystis aeruginosa* in semicontinuous culture. *Limnol. Oceanogr.* 26, 622-634 (1981).

46. Churst, G., Villarino, E., Chenuil, A., Irigoien, X., Bizsel, N., Bode, A., Broms, C., Claus, S., Fernández de Puelles M. L., Fonda-Umani, S. & Hoarau, G. Dispersal similarly shapes both population genetics and community patterns in the marine realm. *Sci. Rep.* 6, 1-12 (2016).

47. Mas, A., Jamshidi, S., Lagadeuc, Y., Eveillard, D. & Vandenkoornhuyse P. Beyond the black queen hypothesis. *ISME J.* 10, 2085-2091 (2012).

48. Amin, S. A., Parker, M. S. & Armbrust, E. V. Interactions between diatoms and bacteria. *Microbiol. Mol. Biol. Rev*. 76, 667-684 (2012).

49. Willey, J. M. & Waterbury, J. B. Chemotaxis toward nitrogenous compounds by swimming strains of marine *Synechococcus* spp. *Appl. Env. Microbiol*. 55, 1888-1894 (1989).

50. Behrenfeld, M. J. & Milligan, A. J. Photophysiological expressions of iron stress in phytoplankton. *Ann. Rev. Mar. Sci*. 5, 217-246 (2013).

51. Halsey, K. H., Milligan, A. J. & Behrenfeld, M. J. Contrasting strategies of photosynthetic energy utilization drive lifestyle strategies in ecologically important picoeukaryotes. *Metabolites* 4, 260-280 (2014).

52. Dortch, Q. Effect of growth conditions on accumulation of internal nitrate, ammonium, amino acids, and protein in three marine diatoms. *J. Exper. Mar. Biol. Ecol.* 61, 243-264 (1982).

53. Dortch, Q., Clayton, J. R., Thoresen, S. S. & Ahmed, S. I. Species differences in accumulation of nitrogen pools in phytoplankton. *Mar. Biol.* 81, 237-250 (1984).

54. Raven, J. A. The role of vacuoles. *New Phytol*. 1, 357-422 (1987).

55. Behrenfeld, M. J., Halsey, K. H., Boss, E., Karp-Boss, L., Milligan, A. J. & Peers, G. Thoughts on the evolution and ecological niche of diatoms. *Ecol. Monogr*. 91, e01457 (2021).

56. Legrand, C., Rengefors, K., Fistarol, G. O. & Graneli, E. Allelopathy in phytoplankton-biochemical, ecological and evolutionary aspects. *Phycologia* 42, 406-419 (2003).

57. Stoecker, D. K., Hansen, P. J., Caron, D. A. & Mitra, A. Mixotrophy in the marine plankton. *Ann. Rev. Mar. Sci*. 9, 311-335 (2017).

58. Lürling, M. Grazing resistance in phytoplankton. *Hydrobiologia*, 848, 237-249 (2021).

59. Harwood, D. M. & Gersonde, R. Lower Cretaceous diatoms from ODP Leg 113 site 693 (Weddell Sea). Part 2: Resting spores, chrysophycean cysts, an endoskeletal dinoflagellate, and notes on the origin of diatoms. In *Proceedings of the Ocean Drilling Program, scientific results*. 113, 403-425 (1990).

60. Rynearson, T. A., Richardson, K., Lampitt, R. S., Sieracki, M. E., Poulton, A. J., Lyngsgaard, M. M. & Perry, M. J. Major contribution of diatom resting spores to vertical flux in the sub-polar North Atlantic. *Deep Sea Res. I* 82, 60-71 (2013).

61. Chesson P. 2000. Mechanisms of maintenance of species diversity. Ann. Rev. Ecol. System. 1; 343-366.

62. Holt, R. D. Predation, apparent competition, and the structure of prey communities. *Theor. Pop. Biol.* 12, 197-229 (1977).

63. Legendre, L. The significance of microalgal blooms for fisheries and for the export of particulate organic carbon in oceans. *J. Plank. Res*. 12, 681-699 (1990).

64. Longhurst, A. R. *Ecological geography of the sea*. Elsevier (2012).

65. Hoopes, M. F., Holt, R. D. & Holyoak, M. The effects of spatial processes on two species interactions. In: *Metacommunities: spatial dynamics and ecological communities* [Hloyoak, Leibod, Holt, eds.], University of Chicago Press, Chicago and London, pp.35-67 (2005).

66. Sommer, U. Algal nutrient competition in continuous culture. *Hydrobiol. Bull*. 17, 21-27 (1983).

67. Smayda, T. J. Biogeographical studies of marine phytoplankton. *Oikos* 9, 158-191 (1958).

68. de Vargas C, et al. Eukaryotic plankton diversity in the sunlit ocean. *Science* 348, 6237 (2015).

69. Balčiūnas, D. & Lawler, S. P. Effects of basal resources, predation, and alternative prey in microcosm food chains. *Ecology* 76, 1327-1336 (1995).

70. W. Fox, J. The dynamics of top-down and bottom-up effects in food webs of varying prey diversity, composition, and productivity. *Oikos* 116, 189-200 (2007).

71. Hiltunen, T., Kaitala, V., Laakso, J. & Becks, L. Evolutionary contribution to coexistence of competitors in microbial food webs. *Proc. Roy. Soc. B: Biol. Sci*. 284, p.20170415 (2017).

72. Lawler, S. P. Direct and indirect effects in microcosm communities of protists. *Oecologia* 93, 184-190 (1993).

73. van der Stap, I., Vos, M., Tollrian, R. & Mooij, W. M. Inducible defenses, competition and shared predation in planktonic food chains. *Oecologia* 157, 697-705 (2008).

74. Holt, R. D. & Bonsall, M. B. Apparent competition. *Ann. Rev. Ecol. Evol. System.* 48, 447-471 (2017).

75. Huntly, N. Herbivores and the dynamics of communities and ecosystems. *Ann. Rev. Ecol. Evol. System.* 22, 477-503 (1991).

76. Terborgh, J. W. Toward a trophic theory of species diversity. *Proc. Nat. Acad. Sci*. 112, 11415-11422 (2015).

77. Ward, B. A., Dutkiewicz, S., Jahn, O. & Follows M. J. A size-structured food-web model for the global ocean. *Limnol. Oceanogr.* 57, 1877-1891 (2012).

78. Moore, D. J. A framework for incorporating ecology into Earth System Models is urgently needed. *Glob. Chang. Biol.* 28, 343-345 (2022).

79. Behrenfeld, M. J. & Boss, E. S. Resurrecting the ecological underpinnings of ocean plankton blooms. *Ann. Rev. Mar. Sci.* 6, 167-194 (2014).

80. Haëntjens, N., Boss, E. S., Graff, J. R., Chase, A. P. & Karp-Boss, L. Phytoplankton size distributions in the western North Atlantic and their seasonal variability. *Limnol. Oceanogr.* 67, 1865-1878 (2022).

FIGURE LEGENDS

Figure 1. Properties of natural phytoplankton populations. (a) Across all open ocean nutrient conditions, phytoplankton populations exhibit continuous size distributions with slopes typically ranging from −3.5 to -4.5 between the logarithm of cell number concentration per unit length and the logarithm of equivalent spherical cell diameter and with steeper slopes observed in more nutrient impoverished waters [12,24]. Division rates are progressively more diffusion-limited as cell size increases. Data shown here were collected in the north Atlantic subtropical gyre [from 80]. (b) Conceptual illustration of the nutrient field experienced by phytoplankton (a 2-dimensional slice through a 3-dimensional field), showing reductions in nutrient concentration through the boundary layers of four, variably-spaced phytoplankton cells being supplied by diffusion of nutrients from the far-field. In nature, cell-to-cell spacing is typically greater than depicted in this figure and far-field nutrient concentrations (S_∞) are not necessarily uniform as in this illustration, but can exhibit short-lived, high-concentration patches resulting from discrete sources of recycled nutrients (e.g., zooplankton excretion).

Figure 2. Lakes as an analogy for nutrient diffusion, the R* rule, and the role of spatial distancing in steady-state plankton systems. (a) The 'Glory Hole' spillway of (b) Lake Berryessa, California. The small spillway can maintain lake levels across its ~80 km^2 surface area because the strong force of gravity rapidly eliminates elevation differences across the lake and the spillway has a high flow capacity. Similarly, phytoplankton cells have the ability to rapidly take up nutrients at their cell surface, creating a strong concentration gradient in their boundary layers. Because diffusion acts to rapidly eliminate concentration differences, the discrete uptake by cells has the potential to rapidly deplete far-field concentrations in the absence of a resupply source. (c) A lake analogy of the R* rule, where the three spillways (A_1, B_1, B_2) represent phytoplankton with different uptake capacities, lake level is initially above all spillways (dashed surface), water drained by the spillways is removed from the system (right pointing arrow exiting drainage system), and there is no new source of water to the lake. Under these conditions, the two B spillways are 'outcompeted' by the A_1 spillway, irrespective of their distancing from A_1, because of the latter's greater drainage ability. In laboratory competition experiments, a superior resource competitor can exclude the inferior competitor, irrespective of distancing between cells, because the former can continue increasing its biomass until the

concentration of limiting resource is sufficiently low that division rate of the inferior competitor is less than the experimentally imposed predation rate. (d) Lake analogy of steady-state plankton systems where water passing through the spillways is redeposited on the lake's surface. In this case, the drawdown potential of the different spillways does not alter the steady-state lake level and, consequently, spatial distancing of spillways $A_1$and B_2 prevents the former from impacting flow through the latter (flow through spillway B_1 is prevented in this depiction because its 'boundary layer' overlaps with that of spillway A_1). In phytoplankton communities, nutrient recycling and spatial distancing similarly allow coexistence of species with vastly different resource uptake potentials. These analogies are intended to provide intuition regarding plankton systems, rather than a robust depiction of the three-dimensional space defining growth conditions of phytoplankton cells.

Figure 3. Predictions of phytoplankton community properties and resource distributions from a one-dimensional ecosystem model. (a) Relationship between nitrogen inventory (ΣN), far-field nitrogen concentration (S_∞; blue line), and steady-state nitrogen resupply rate (orange line). Dashed green lines bracket typical nitrogen S_∞ values for oligotrophic ocean gyres. (b) Phytoplankton size distributions (blue line) (logarithm of cell number concentration per unit length versus logarithm of cell diameter) become increasingly steep as ΣN decrease from 20 to 4 μM, but all 25 phytoplankton size classes included in model initiations are retained at steady state (orange line) for all values of ΣN. (c) Steady-state partitioning of nitrogen inventories between phytoplankton (blue line), zooplankton (orange line), and dissolved (green line) pools. For $\Sigma N < 10$ μM, nearly all of the resource is sequestered in phytoplankton and zooplankton biomass (gray line). See **METHODS** and Behrenfeld et al. [19] for model details.

Figure 4. Depiction of the multi-dimensional trade-space available to phytoplankton for achieving equivalent fitness within predator-prey created ecological niches. In this schematic, phytoplankton species have twelve investment options indicated by nodes (black labeled squares) that are evenly distributed across the surface of the trade-space volume. Any location within this volume (infinite options) is a valid solution for achieving equal fitness in an ecological niche, but the actual positions of extent coexisting species are defined by evolved investment strategies. For example, species A (red sphere) is positioned within the trade-space

602 volume closer to defense-related investment options [e.g., vectors (red dotted lines) connecting
603 to armory, predator avoidance, chemical defense], implying a competition solution focused on
604 reducing the loss term in the predator-prey balance (i.e., μ - l). Species B (green sphere), on the
605 other hand, is positioned closer to resource relevant nodes [e.g., vectors (green dotted lines)
606 connecting to resource affinity, cell quota, opportunistic physiology], implying investments
607 focused more on the division element (μ) of the predator-prey balance. As described in the text,
608 each investment option identified in this figure may have multiple forms [e.g., 'opportunistic
609 physiology' could include chemotaxis, excess photosynthetic capacity, luxury nutrient uptake,
610 enhanced division rate maxima, among others], and the full suite of options available to
611 phytoplankton likely exceeds the twelve shown here. A phytoplankton species might also invest
612 in only a subset of these options, such as a 'defense specialist' investing in armor and predator
613 avoidance (e.g., swimming) and neglecting investment in chemical defenses.

Figure 1

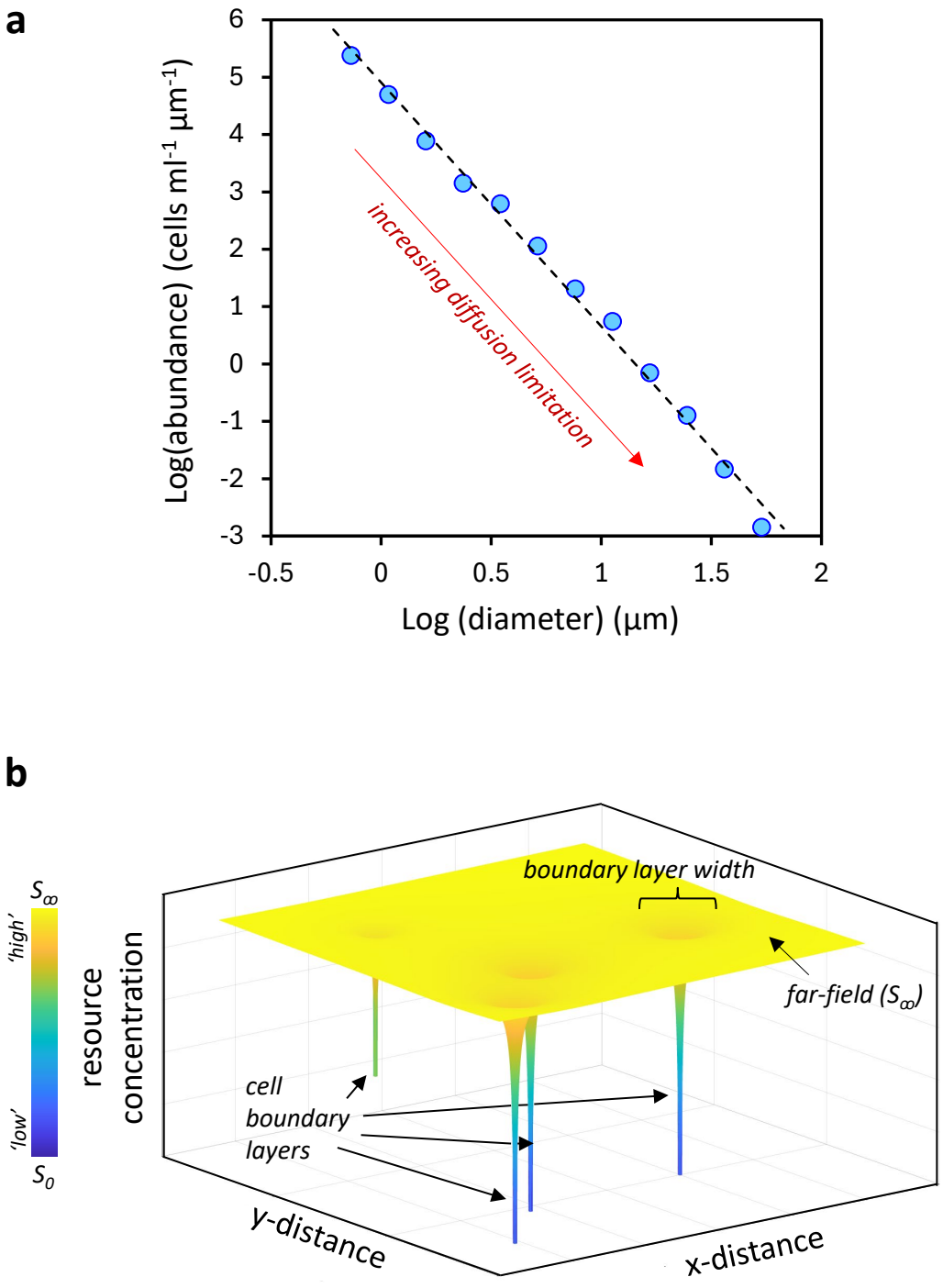
a
Log(abundance) (cells ml-1 µm-1)
6
5
4
3
2
1
0
-1
-2
-3
-0.5
0
0.5
1
1.5
2
Log (diameter) (µm)
increasing diffusion limitation
b
resource concentration
S∞
'high'
'low'
S0
boundary layer width
far-field (S∞)
cell boundary layers
y-distance
x-distance

Figure 2

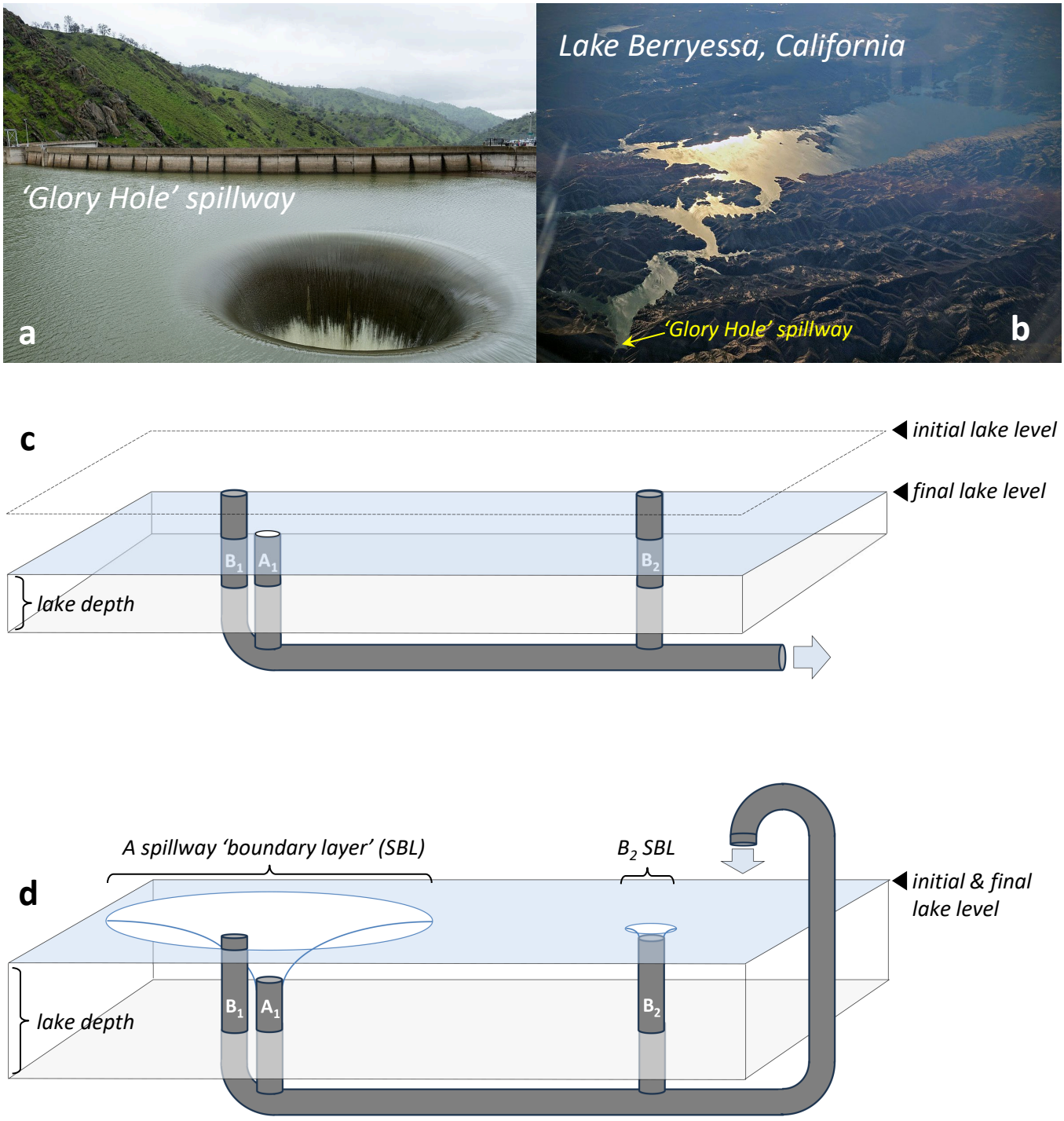
'Glory Hole' spillway
a
Lake Berryessa, California
'Glory Hole' spillway
b
c
initial lake level
final lake level
B1
A1
B2
lake depth
d
A spillway 'boundary layer' (SBL)
B2 SBL
initial & final
lake level
B1
A1
B2
lake depth

Figure 3

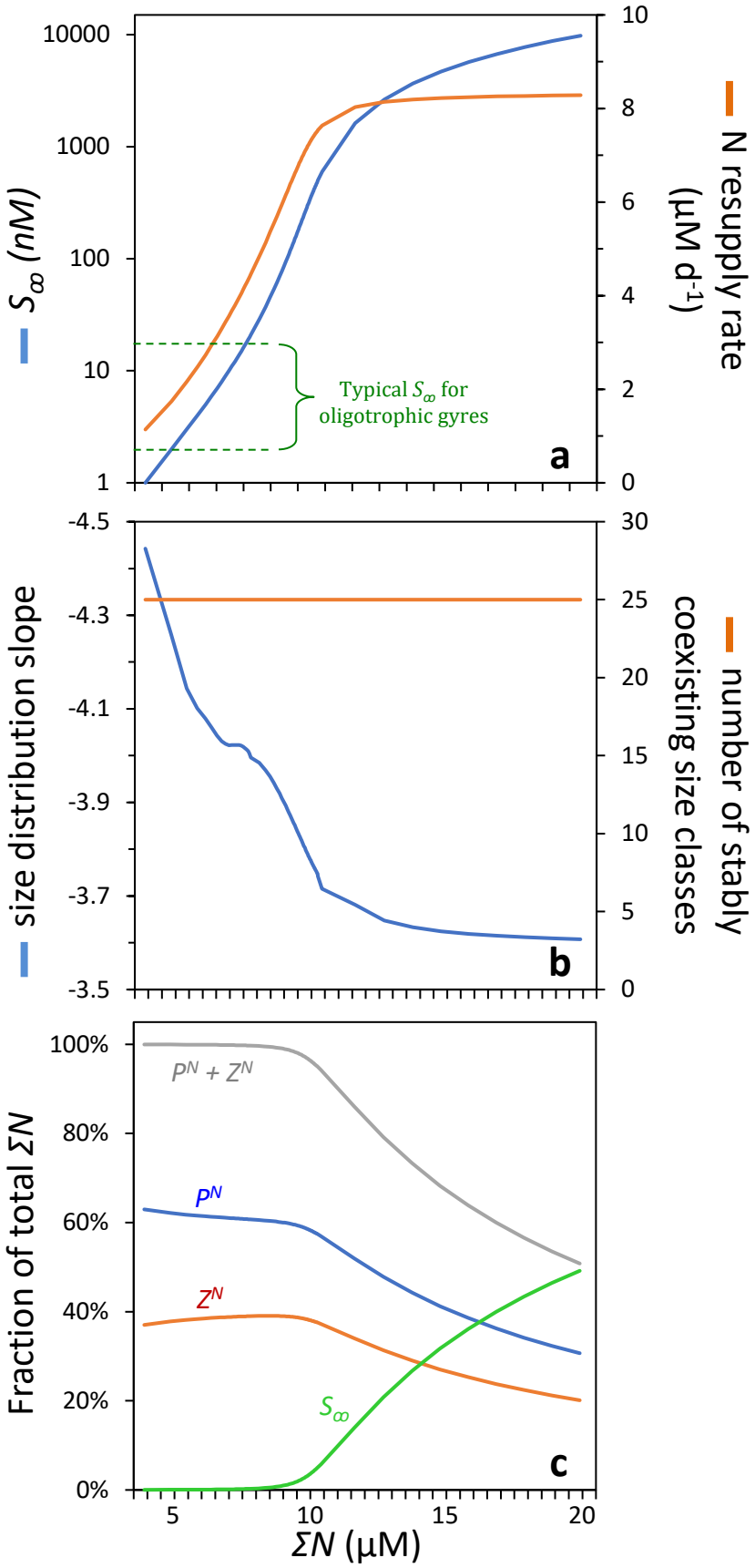
10000
1000
100
10
1
S_∞ (nM)
10
8
6
4
2
0
N resupply rate (μM d^{-1})
Typical S_∞ for oligotrophic gyres
a
-4.5
-4.3
-4.1
-3.9
-3.7
-3.5
size distribution slope
30
25
20
15
10
5
0
number of stably coexisting size classes
b
100%
80%
60%
40%
20%
0%
Fraction of total ΣN
$P^N + Z^N$
P^N
Z^N
S_∞
c
5
10
15
20
ΣN (μM)

Figure 4

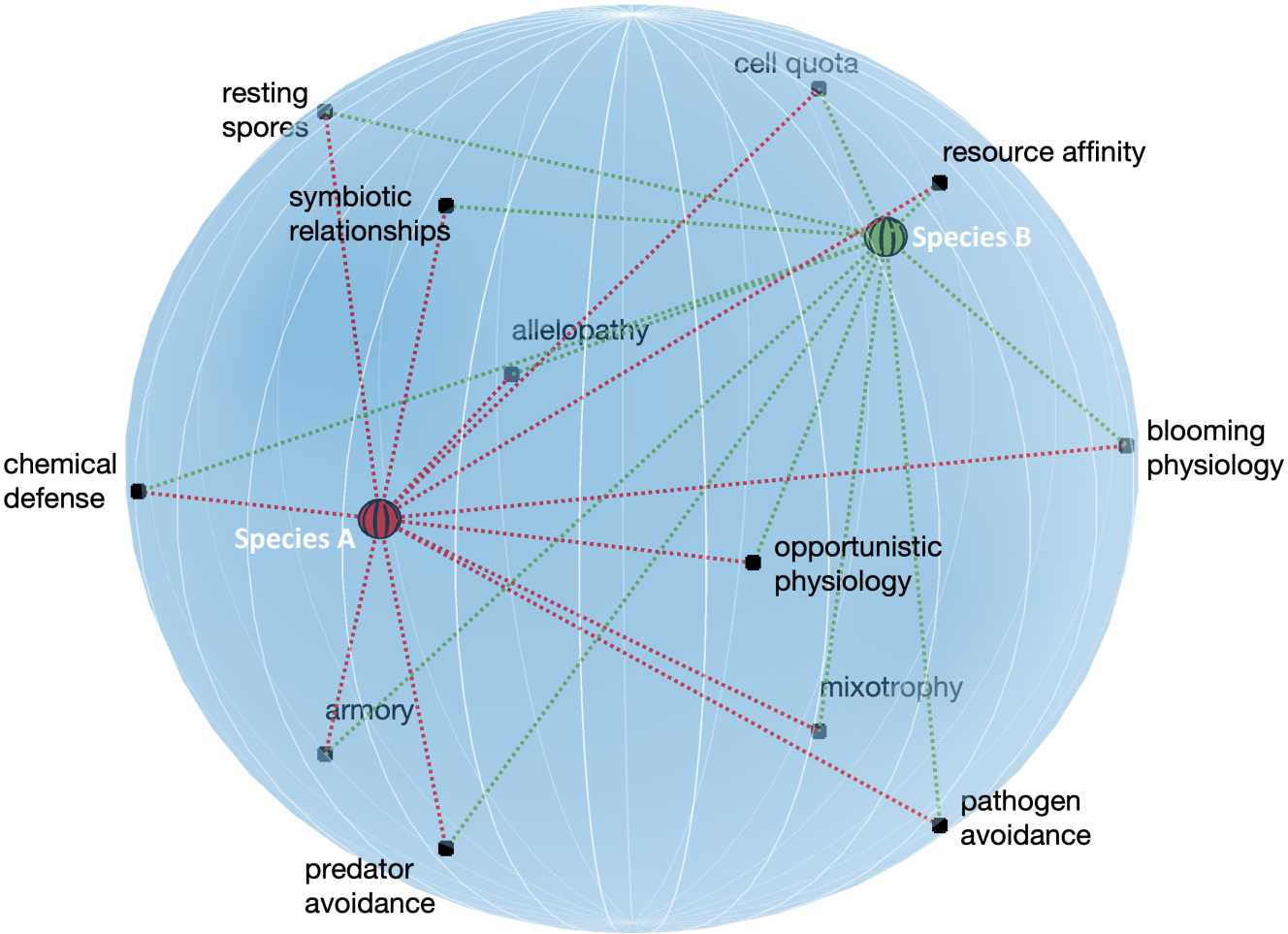
cell quota
resting spores
resource affinity
symbiotic relationships
Species B
allelopathy
chemical defense
blooming physiology
Species A
opportunistic physiology
mixotrophy
armory
pathogen avoidance
predator avoidance

Supporting Information

Phytoplankton competition, cell-to-cell spacing, and biodiversity

This PDF file includes:

SUPPORTING DISCUSSION

The time required for a population of like-sized phytoplankton to reduce far-field nutrient concentrations (S_∞) by one half ($t_{1/2}$) in the absence of any new source of that nutrient is dependent of cell properties (size, motility, etc.), cell abundance, maximum division rate (i.e., the degree to which division is saturated by the diffusion of limiting resource), and the concentration gradient between the cell surface and the far-field. To estimate size-dependent $t_{1/2}$ values for representative natural phytoplankton populations, we assumed a phytoplankton size distribution with a -4.4 slope between the logarithm of cell number concentration per unit length and the logarithm of cell diameter. $t_{1/2}$ values were estimated for cell diameters of 0.6, 1.5, 2.5, 4, 8, 16, 30, 50, 70, 100, and 130 µm and a range in S_∞ of 1 nM to 10 µM (in steps of 1 nM from 1 to 21 nM, ~ 8 nM from 21 to 500 nM, and ~ 1 µM from 1 to 10 µM). The smallest size class represents *Prochlorococcus*, which typically exhibits cell concentrations ranging from 2×10^4 to 2×10^5 cell ml^{-1} in natural oligotrophic waters [Behrenfeld et al. 2022]. Inorganic nitrogen concentrations (S_∞) in these waters typically range from 3 to 17 nM. Since the predator-prey determined steady-state in phytoplankton concentration increases with increasing division rate [Behrenfeld & Boss 2014, 2018], we assumed *Prochlorococcus* concentrations to increase linearly from 2×10^4 to 2×10^5 cell ml^{-1} as S_∞ increases from 1 to 17 nM. Division rate (μ) for each phytoplankton size class was calculated as a size-dependent saturating function of S_∞ defined by diffusion rate and maximum potential μ, as described in detail in Behrenfeld et al. [2022]. For these calculations, we also assumed that all phytoplankton were motile and non-vacuolated (i.e., non-diatoms) [Behrenfeld et al. 2022].

Supporting Information Figure 1 shows the resultant relationships between $t_{1/2}$ and S_∞ from the calculations described above. We call attention to a variety of aspects regarding these results. First, $t_{1/2}$ for oligotrophic gyre conditions (green shading) ranges from ~1 day to > 1 year for all size classes ≥ 1.5 µm [i.e., *Synechococcus* (d = 1.5 µm) and larger]. Only *Prochlorococcus* has a $t_{1/2}$ < 1 day in these waters. Second, for S_∞ < 17 nM, $t_{1/2}$ increases with increasing S_∞ for all size classes ≥ 1.5 µm, which is a consequence of both the assumed increase in cell abundance as S_∞ increases from 1 to 17 nM and the increasing concentration gradient from the cell surface (S_0) to the far-field (S_∞). In contrast, $t_{1/2}$ for *Prochlorococcus* decreases over essentially the full range of

S_∞, despite increases in cell numbers from S_∞ of 1 to 17 nM. The reason for this decrease is that division rates for *Prochlorococcus* are nearly saturated by diffusion at even the lowest S_∞ [Behrenfeld et al. 2022] and the assumed increase in cell abundance over the oligotrophic range in S_∞ is not sufficient to overcome the longer time requirement for an essentially constant uptake rate to deplete far-field nutrients by 50% (note that this saturation of division by diffusion is also apparent in the shouldering of $t_{1/2}$ for *Synechococcus* as S_∞ approaches 17 nM and the shouldering of $t_{1/2}$ for larger cells at $S_\infty > 17$ nM). Third, diffusion rates described in Behrenfeld et al. [2022] assume that each cell in each size class can achieve the theoretical maximum μ. Because measured maximum μ values for many phytoplankton species fall below these theoretical limits, our calculated $t_{1/2}$ values (Supporting Information Fig. 1) will tend to be underestimated. On the other hand, concentrations of larger cells tend to increase in nature as S_∞ increases, causing the slope of the size distribution to be greater than -4.4 and implying somewhat smaller $t_{1/2}$ for these larger cells at high S_∞. Finally, Ward [2024] reported a $t_{1/2}$ value for *Prochlorococcus* of 22 minutes, which is much faster than our values. The reason for this discrepancy is that the former study assumed a fixed concentration of *Prochlorococcus* at 10^5 cells ml^{-1} and unrestricted uptake by diffusion. If we adopt these same assumptions in our calculations, we get the very comparable estimate of $t_{1/2} = 23$ minutes, illustrating the significance of our more realistic assessments of cell abundance and saturation of division by diffusive flux.

REFERENCES

Behrenfeld, M. J. & Boss, E. S. Resurrecting the ecological underpinnings of ocean plankton blooms. *Ann. Rev. Mar. Sci.* 6, 167-194 (2014).

Behrenfeld, M. J. & Boss, E. S. Student's tutorial on bloom hypotheses in the context of phytoplankton annual cycles. *Global Change Biol*. 24, 55-77 (2018).

Behrenfeld M. J., Bisson, K. M., Boss, E., Gaube, P. & Karp-Boss, L. Phytoplankton community structuring in the absence of resource-based competitive exclusion. *Plos one* 17, e0274183 (2022).

Ward, B. A. How phytoplankton compete for nutrients despite vast intercellular separation. *ISME Comm.* 4, p.ycae003 (2024).

SUPPORTING INFORMATION FIGURE S1

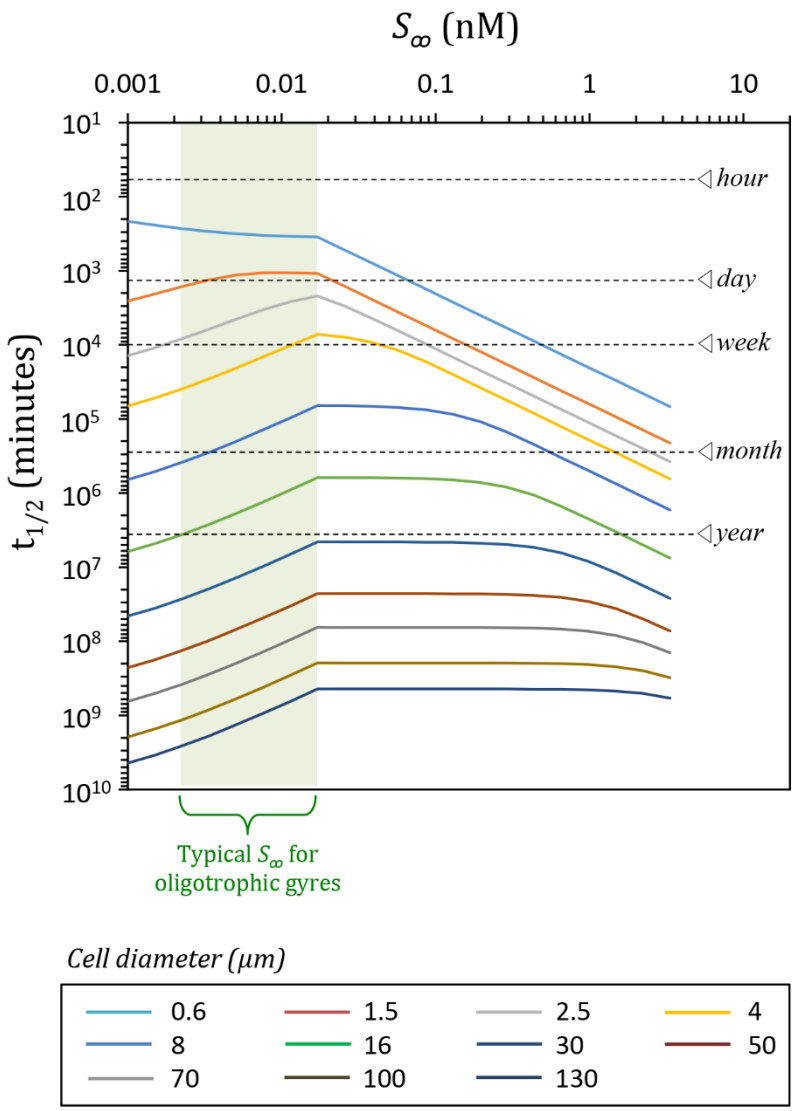

Figure S1. Nutrient depletion potentials as a function of far-field nutrient concentration (S_∞). Time required ($t_{1/2}$) for a 50% reduction in S_∞ for phytoplankton with cell diameters (spherical equivalents) ranging from 0.6 to 130 µm (coloring defined in box), assuming no new input of limiting resource. Green shading = typical nitrogen concentrations in oligotrophic ocean gyres. See Supporting Discussion for details on calculations and discussion of features in the graph.